Chaos

Temporal evolution of failure avalanches of the fiber bundle model on complex networks

Cite as: Chaos **32**, 063121 (2022); https://doi.org/10.1063/5.0089634
Submitted: 27 February 2022 • Accepted: 20 May 2022 • Published Online: 10 June 2022

Attia Batool, Zsuzsa Danku, Gergő Pál, et al.

AIP Publishing

Temporal evolution of failure avalanches of the fiber bundle model on complex networks

Cite as: Chaos **32**, 063121 (2022); doi: 10.1063/5.0089634
Submitted: 27 February 2022 · Accepted: 20 May 2022 ·
Published Online: 10 June 2022

Attia Batool,[1] Zsuzsa Danku,[1] Gergő Pál,[1] and Ferenc Kun[1,2,a)]

AFFILIATIONS

[1]Department of Theoretical Physics, Doctoral School of Physics, Faculty of Science and Technology, University of Debrecen, P.O. Box 400, H-4002 Debrecen, Hungary
[2]Institute of Nuclear Research (Atomki), Poroszlay út 6/c, H-4026 Debrecen, Hungary

[a)]**Author to whom correspondence should be addressed:** ferenc.kun@science.unideb.hu

ABSTRACT

We investigate how the interplay of the topology of the network of load transmitting connections and the amount of disorder of the strength of the connected elements determines the temporal evolution of failure cascades driven by the redistribution of load following local failure events. We use the fiber bundle model of materials' breakdown assigning fibers to the sites of a square lattice, which is then randomly rewired using the Watts–Strogatz technique. Gradually increasing the rewiring probability, we demonstrate that the bundle undergoes a transition from the localized to the mean field universality class of breakdown phenomena. Computer simulations revealed that both the size and the duration of failure cascades are power law distributed on all network topologies with a crossover between two regimes of different exponents. The temporal evolution of cascades is described by a parabolic profile with a right handed asymmetry, which implies that cascades start slowly, then accelerate, and eventually stop suddenly. The degree of asymmetry proved to be characteristic of the network topology gradually decreasing with increasing rewiring probability. Reducing the variance of fibers' strength, the exponents of the size and the duration distribution of cascades increase in the localized regime of the failure process, while the localized to mean field transition becomes more abrupt. The consistency of the results is supported by a scaling analysis relating the characteristic exponents of the statistics and dynamics of cascades.

Cascading failure driven by the redistribution of load after local damage events of connected elements often occurs in our technological environment. From the cascading blackouts of electric transmission grids, through the failure avalanches of transportation and communication networks to the crackling bursts accompanying the breakdown of materials, a large variety of failure phenomena can be mentioned that often have a strong economic impact. Here, we investigate how the interplay of the topology of the network of load transmitting connections and the randomness of the strength of the connected elements governs the temporal evolution of failure cascades. Based on computer simulations of a generic model of failure spreading, we determine the average temporal profile of avalanches and explore how the shape of the profiles evolves as the structural randomness of the underlying network and the amount of disorder of node strength are varied.

I. INTRODUCTION

Avalanching or cascading dynamics, where a local event of activity triggers a sequence of events, is a common feature of a broad variety of complex systems.[1–4] Examples range from the epidemic spreading on social networks,[5–9] through the avalanche activity of neural networks[10] to the crackling bursts accompanying the fracture of heterogeneous materials[11–14] up to the length scale of earthquakes.[15] The statistics of the size (magnitude) of avalanches has been extensively studied as a primary source of information on the intermittent dynamics of complex systems.[10,16] Recently, it has been demonstrated in the field of Barkhausen noise of ferromagnetic materials[17] and in fracture processes[18] that the temporal profile of avalanches provides a deeper insight into the underlying dynamics of avalanche formation. Careful experiments revealed that Barkhausen avalanches have a parabolic profile with a left handed asymmetry.[19] Subsequent theoretical investigations clarified both

the origin of asymmetry and the scaling relations of the characteristic quantities of avalanche profiles and the statistics of the size and duration of avalanches.[19–21] Recently, it has been shown for models of the spreading of diseases and information, furthermore, for the activity patterns of neural networks that the avalanche profiles are sensitive to the topology of the contact network of the elements of the system.[9] In particular, the degree distribution of the network proved to play a crucial role in the temporal evolution of cascades. A parameter regime of network topologies could be identified where the Markovian dynamics of spreading leads to parabolic avalanche profiles with a left handed asymmetry.[9]

Cascading failure driven by the redistribution of load following the local damage of connected elements often occurs in our technological environment, e.g., in the case of the cascading blackouts of electric transmission grids[2] or in the breakdown of communication and transportation networks.[8–10,22–25] Failure cascades form a distinct class of cascading activities in the sense that as the cascade spreads, elements of the system become irreversibly inactive without any further ability to support load. The reduction of the load bearing capacity together with the constraint of load conservation can easily give rise to large scale breakdown events spanning a macroscopic fraction of the system.[24–29] The statistical features of such failure cascades have recently been studied using discrete models;[24,25] however, much less is known about their temporal evolution and its dependence on the structure of the underlying network.

Here, we use the fiber bundle model (FBM) to investigate how the interplay of the structure of the underlying network of load transmitting connections and the amount of disorder of the load bearing capacity (strength) of the nodes determines the dynamics of failure avalanches and the relation of their dynamical and statistical features. In spite of their simplicity, FBMs of materials breakdown have proven very useful in studying cascading failure phenomena since the model is able to capture the essential mechanisms of intermittent failure spreading.[3,27,28,30] In the standard setup, FBMs are composed of a set of parallel fibers organized on a regular lattice. Under a slowly increasing external load, the fibers fail irreversibly when the local load on them exceeds their strength value, which is assumed to have a certain amount of randomness. The load dropped by the broken fiber gets redistributed over the remaining intact ones, which may trigger additional breakings giving rise to the emergence of an extended failure cascade. The generality of this spreading mechanism makes FBMs a basic modeling framework for cascading failure[29,31–33] since fibers can easily be replaced by electric power stations[2,34–36] on a high voltage transmission grid, by flow channels,[37] or by roads carrying traffic.[38,39] In our study, the complex network of load transmitting connections is obtained by assigning fibers to the sites of a square lattice which is then randomly rewired using the Watts–Strogatz technique.[40] Gradually increasing the rewiring probability, we demonstrate that the bundle undergoes a transition from the localized to the mean field universality class of breakdown phenomena. Computer simulations revealed that both the size and the duration of failure avalanches are power law distributed on all network topologies with a crossover between two regimes of different exponents. The temporal evolution of cascades is described by a parabolic profile with a right handed asymmetry, which implies that avalanches start slowly, then accelerate, and eventually stop suddenly. The degree of asymmetry proved to be characteristic of the network topology.

II. FIBER BUNDLE MODEL ON COMPLEX NETWORKS

To study the spreading of failure cascades, we consider a bundle of parallel fibers that are assigned to the nodes of a complex network. To generate the network of connections along which load is redistributed over fibers, we start from a regular square lattice of side length l with $N = l^2$ fibers and use the Watts–Strogatz rewiring technique to randomize the connections.[40,41] The degree k_i of node i ($i = 1, \ldots, N$), is defined as the number of interacting partners (nodes) directly connected to i through links of the networks. Initially, on the square lattice, all fibers are connected to their four nearest neighbors along the edges of the lattice so that the probability distribution of the node degree $\rho(k)$ has the simple form $\rho(k) = 1$ for $k = 4$, and it is zero for any other k value. In the next step, each of the $L = 2N$ initially existing connections is rewired with a probability p ($0 \leq p \leq 1$) in such a way that for both ends of a rewired link, a new fiber is selected randomly. In order to ensure that the network forms a simple graph, rewiring is subject to the constraint that neither multiple links nor loops are allowed (see Fig. 1 for illustration of the model construction). These randomized connections make the degree distribution $\rho(k)$ broader while the average degree of nodes $\langle k \rangle$ remains fixed $\langle k \rangle = 4$. The evolution of the degree distribution $\rho(k)$ of the bundle with increasing rewiring probability is illustrated in Fig. 2. Note that the functional form of the degree distribution $\rho(k)$ obtained by the rewiring algorithm can be described as the convolution of a binomial and a Poissonian distribution.[42] At high values of p close to 1, small clusters composed of a few fibers may form as a consequence of rewiring. To start the simulations

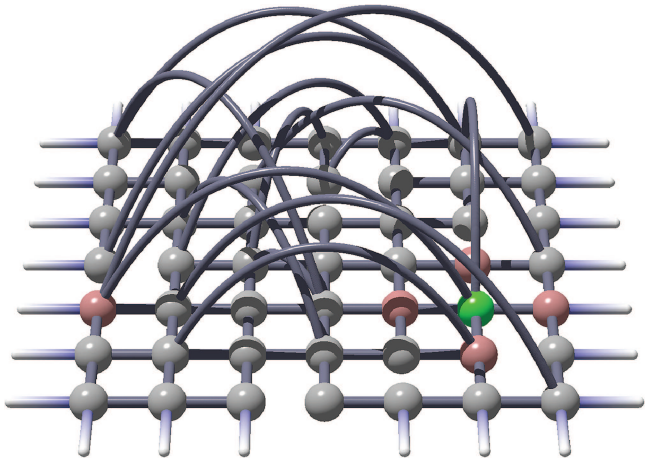

FIG. 1. Illustration of the model construction. A regular square lattice is gradually randomized by means of the Watts–Strogatz rewiring technique. Periodic boundary conditions are applied in both directions of the initial lattice. Links of the network represent the load transmitting connections of fibers, which are perpendicular to the plane of the lattice.

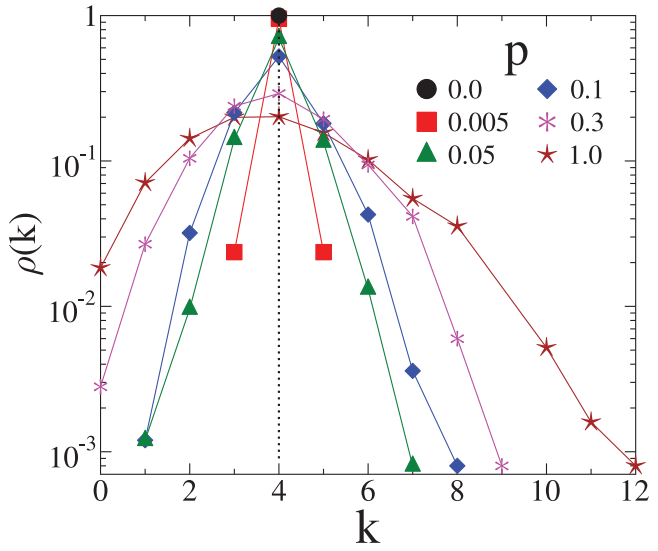

FIG. 2. Degree distribution of the network of fibers at several rewiring probabilities p. As p increases the distribution $\rho(k)$ gets broader, however, the average degree remains constant $\langle k \rangle = 4$.

with a fully connected network, after rewiring, we identify all clusters of nodes in the system and keep only the largest one for further calculations.

The fibers of the model have a linearly elastic behavior up to a threshold load σ_{th}, where they fail irreversibly. We assume that the Young modulus of fibers is the same as $E = 1$; however, their strength σ_{th} is a random variable with the probability distribution $p(\sigma_{th})$. In the present study, the breaking thresholds are sampled from a Weibull distribution,

$$p(\sigma_{th}) = m\frac{\sigma_{th}^{m-1}}{\lambda^m}e^{-(\sigma_{th}/\lambda)^m}, \tag{1}$$

defined over the range $0 \leq \sigma_{th} < +\infty$. The distribution has two parameters λ and m such that λ sets the scale of strength values, while m controls the functional form of the distribution. The Weibull distribution Eq. (1) has two main advantages for our study: on one hand, the fracture behavior of FBMs with such a fast decaying strength distribution exhibits a high degree of universality, which has been extensively studied on regular square lattices during the past few decades.[28,43] On the other hand, the Weibull distribution makes it possible to vary the amount of disorder of the failure thresholds, i.e., increasing the parameter m in the range $m \geq 1$ the width of the distribution, and hence, the variance of fibers' strength, decreases and tends to zero in the $m \to \infty$ limit. In our model construction, the strength σ_{th}^i and degree k_i of fibers $(i = 1, \ldots, N)$ are uncorrelated.

To initiate the breakdown process, the bundle is subject to a slowly increasing external mechanical load, which generates a homogeneous stress field until the weakest fiber with the lowest failure threshold breaks. The load of the broken fiber has to be redistributed over the surviving intact ones. Recently, two limiting cases of load sharing have been extensively studied both with a high theoretical and practical relevance: in the case of equal load sharing (ELS), all the intact fibers share equally the excess load,[27,28] while for localized load sharing (LLS), the intact nearest neighbors take over equally the load of the broken one.[43–45] ELS realizes the mean field limit of fiber bundles since under such conditions, no stress fluctuations can arise in the system. However, for LLS, a strong load concentration emerges around failed regions. Here, we apply nearest neighbor interaction so that the load dropped by the broken fiber is equally shared by its intact nearest neighbors on the network: when fiber i of load σ_i fails during the loading process, then its n_i intact nearest neighbors all receive the load increment $\Delta\sigma_i = \sigma_i/n_i$ so that the load σ_j of a neighboring fiber j is updated as

$$\sigma_j \to \sigma_j + \Delta\sigma_i. \tag{2}$$

The number of intact nearest neighbors n_i can be obtained from the adjacency matrix A of the network as

$$n_i = \sum_{j=1}^{N} A_{ij}, \tag{3}$$

where $A_{ij} = 1$ if fibers i and j are connected and they are both intact, and 0 otherwise. As a consequence of load sharing, the load of the neighboring fibers may exceed their local breaking threshold resulting in additional breakings, which are then followed again by load redistribution. As a result of subsequent breaking and load redistribution steps, a single fiber breaking may trigger an entire cascade of failures. The cascade stops when all the fibers receiving load in a redistribution step can sustain the increased load. During an avalanche, the external load is kept constant so that the failure spreading is solely driven by the redistribution of load through the transmission network. Localized load sharing implies that the fibers breaking in an avalanche form a connected cluster on the load transmission network in such a way that on the intact fibers along the cluster perimeter a large amount of load can accumulate.

To ensure quasi-static loading of the bundle, after an avalanche stops, the external load is increased again to break a single fiber so that the load σ_i of each intact fiber is incremented by the same amount $\delta\sigma$,

$$\sigma_i \to \sigma_i + \delta\sigma, \tag{4}$$

where $\delta\sigma$ is determined as the smallest difference between the load σ_i and strength σ_{th}^i of intact fibers $\delta\sigma = \min_i(\sigma_{th}^i - \sigma_i)$. The ultimate failure of the system occurs when a load increment triggers a catastrophic cascade breaking all the intact fibers.

Simulations of the failure dynamics were performed starting from a square lattice of size $l = 400$ with $N = 160\,000$ fibers using periodic boundary conditions in both directions. The scale parameter of the disorder distribution λ was fixed to $\lambda = 1$, while the Weibull exponent m was varied in the range $1 \leq m \leq 15$. For the rewiring probability p, we considered 30 different values in the interval $0 \leq p \leq 1$. At each parameter set, averages were calculated over 2000 samples.

III. STATISTICS OF CASCADE SIZE AND DURATION

The microscopic mechanism of failure of the system is the cascading breaking of fibers triggered by external load increments. The

quasi-static loading ensures that a cascade always starts from a single breaking fiber. After load redistribution, additional fibers of number Δ_s may break, which defines a sub-cascade of the evolving cascade. To characterize single cascades, we determined their size Δ as the total number of fibers breaking in the cascade and the duration (or width) W, which is the number of breaking—load redistribution steps performed until the cascade stops. The size Δ of a cascade, the size Δ_s of its sub-cascades, and the duration W of the event are related as

$$\Delta = \sum_{u=1}^{W} \Delta_s(u), \tag{5}$$

where u is the internal time variable of a cascade (or simply the integer index of sub-cascades).

As a cascade grows, it spreads over the transmission network, which is demonstrated in Fig. 3 for an event of size $\Delta = 84$ and duration $W = 24$. In the figure, fibers breaking in a sub-cascade are indicated by the same color so that starting from the externally imposed fiber breaking, one can easily follow the development of the cascade through the consecutive sub-cascades (colors). Note that fibers breaking in the same sub-cascade can be far from each other, however, the entire cascade forms a connected cluster on the network. The inset demonstrates how the size of sub-cascades Δ_s evolves as the cascade is spreading on the network.

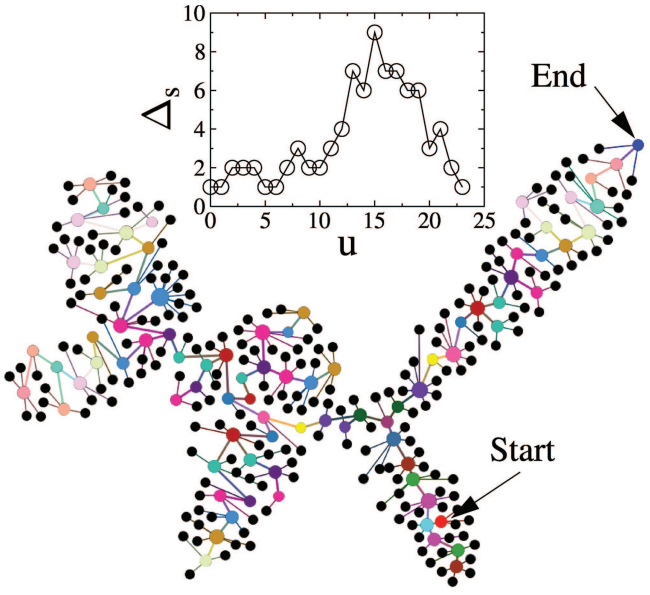

FIG. 3. Spreading of a failure cascade on the network of load sharing connections. The cascade starts and ends with a single breaking indicated by the arrows. All fibers of the network that receive a load from broken fibers are indicated by black circles and among them, the ones which break as a consequence of load sharing are highlighted by colors different from black. For clarity, the circles representing broken fibers have also a larger size. Fibers breaking in the same sub-cascade have the same color. The cascade in the example has the size $\Delta = 84$ and duration $W = 24$. The inset presents the temporal profile $\Delta_s(u)$ of the avalanche.

To characterize the statistics of the occurrence of cascades, first we determined the probability distribution of their size $p(\Delta)$, which proved to depend on the network topology of load transmitting connections. On the regular square lattice $p = 0$ where strong spatial localization of load occurs around broken clusters all the cascades are typically small compared to the system size N, because large cascades easily become catastrophic destroying the entire system. Figure 4 demonstrates for the Weibull parameter $m = 3$ that at $p = 0$ the size distribution $p(\Delta)$ can be well approximated as a power law,

$$p(\Delta) \sim \Delta^{-\tau}, \tag{6}$$

where the value of the exponent τ proved to be relatively high $\tau = 4.7 \pm 0.15$ in agreement with former fiber bundle studies.[44,46] At higher rewiring probabilities p, the growing fraction of long range connections reduces the load concentration, which allows the bundle to tolerate larger failure cascades without catastrophic failure. Consequently, in Fig. 4, the cutoff burst size $\Delta_{\max}$ increases, and the distribution $p(\Delta)$ undergoes a crossover to a second power law regime with a lower exponent. Due to the increasing fraction of larger avalanches emerging in the failure dynamics, the value of the exponent τ gets gradually lower with increasing p. The crossover burst size Δ_c depends on the rewiring probability in such a way that with increasing p, the value of Δ_c shifts to smaller values. It can be observed in Fig. 4 that in the limit $p \to 1$, only a single power law prevails with an exponent $\tau = 2.3 \pm 0.1$ significantly lower than that of the original square lattice.

Usually, the duration of an avalanche is smaller than its size $W \leq \Delta$, where equality holds only when in all sub-cascades, a single fiber breaks. It can be seen in Fig. 5 for the same parameters as in Fig. 4 that the distribution of the duration of failure cascades $p(W)$

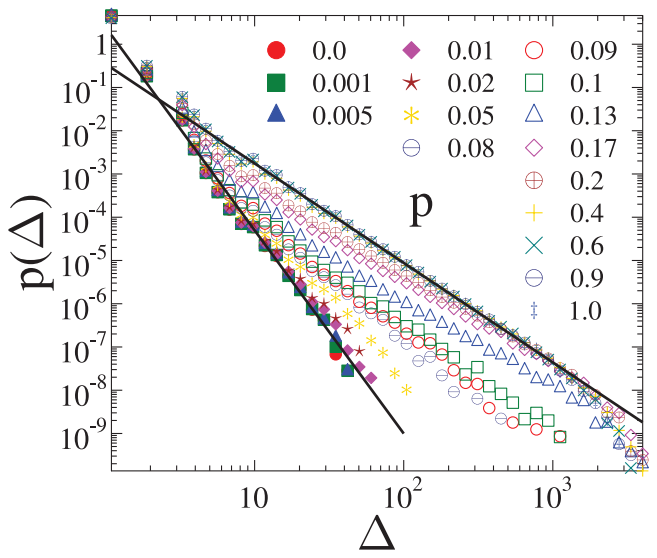

FIG. 4. The size distribution of failure cascades $p(\Delta)$ at different rewiring probabilities p at the Weibull parameter $m = 3$. The two straight lines represent power laws of exponents 2.3 and 4.7.

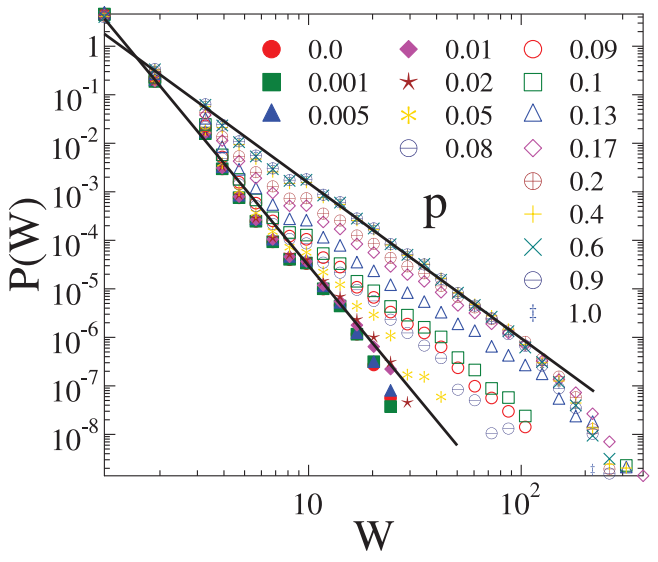

FIG. 5. The distribution of the duration of failure cascades $p(W)$ for the same Weibull exponent m as in Fig. 4. As p increases, a crossover emerges between two power law regimes of different exponents similar to the behavior of the size distribution $p(\Delta)$. The two straight lines represent power laws of exponents 3.2 and 5.3.

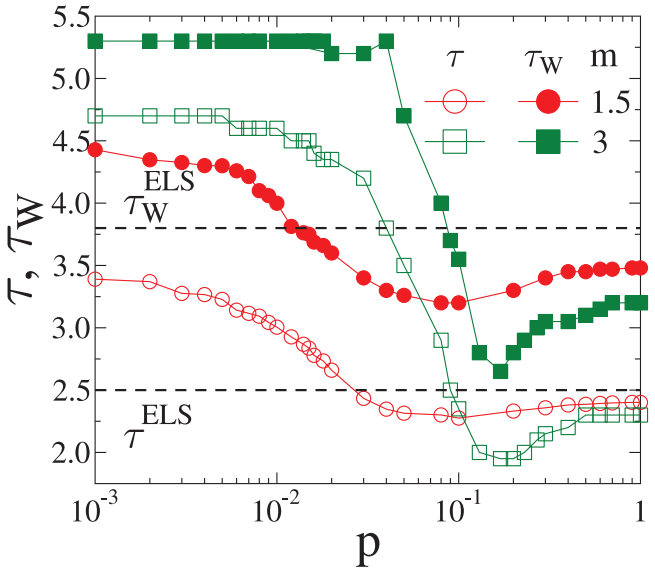

FIG. 6. The power law exponents τ and τ_W of the probability distributions of the size $p(\Delta)$ and duration $p(W)$ of failure cascades as a function of the rewiring probability p for two different Weibull exponents m. The horizontal dashed lines represent the mean field values τ^{ELS} and τ_W^{ELS} of the two exponents.

has qualitatively the same behavior as the cascade size distribution $p(\Delta)$ when the rewiring probability p is varied: for the regular lattice $p = 0$, a power law distribution is evidenced

$$p(W) \sim W^{-\tau_W}, \tag{7}$$

with a relatively high exponent $\tau_W \approx 5.3$ showing that avalanches of long duration rarely occur during the failure process. When long range connections are introduced, the system can survive larger avalanches of longer duration, hence, with increasing p a crossover emerges between two regimes of different exponents. The crossover duration W_c decreases with increasing p so that in the limit $p \to 1$, the crossover gradually disappears and a single power law prevails with an exponent $\tau_w \approx 3.2$, which is significantly smaller than the one of the regular lattice. It is important to note that the exponent τ_W of the duration distribution is always higher than the size distribution exponent τ.

To give a detailed characterization of the evolution of the statistics of the size and duration of failure cascades as the network is gradually randomized, we determined the average of the largest size $\langle \Delta_{\max} \rangle$ and the largest duration $\langle W_{\max} \rangle$ of cascades; furthermore, the power law exponents τ and τ_W of the distributions in the regime of large avalanches as a function of the rewiring probability p for two values of the Weibull exponent $m = 1.5, 3$. It can be observed in Figs. 6 and 7 that up to a threshold value of the rewiring probability $p_l(m)$ all the characteristic quantities τ, τ_W, $\langle \Delta_{\max} \rangle$, and $\langle W_{\max} \rangle$ are nearly constant keeping their $p = 0$ values, which implies that in the parameter range $p \lesssim p_l$ the small fraction of randomized contacts have a minor effect on failure avalanches. However, above this threshold probability, the failure dynamics rapidly changes indicated by the steep increase of both the cutoff size $\langle \Delta_{\max} \rangle$ and duration $\langle W_{\max} \rangle$ of cascades (Fig. 7), and by the rapidly decreasing exponents τ and τ_w of the distributions (Fig. 6). For high rewiring probabilities $p \to 1$, the exponents τ and

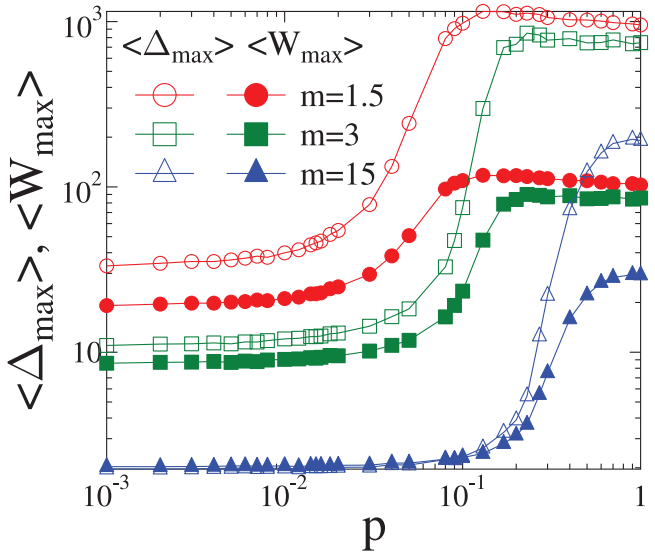

FIG. 7. The average of the largest burst size $\langle \Delta_{\max} \rangle$ and largest duration $\langle W_{\max} \rangle$ as a function of the rewiring probability p for three different values of the Weibull exponent m.

τ_w both converge to constants $\tau \approx 2.3$–2.4 $\tau_W \approx 3.2$–3.5, which fall very close to their corresponding mean field values $\tau^{ELS} = 5/2$ and $\tau_W^{ELS} \approx 3.8$. The results show that on sufficiently randomized load transmission networks, the statistics of the size and duration of failure cascades of the localized load sharing FBM becomes equivalent to the mean field (ELS) universality class of the system. Gradually increasing the rewiring probability an LLS to ELS transition emerges, which sets on at the threshold value p_l and gets completed at the upper bound p_u of the rewiring probability beyond which no significant change of the characteristic quantities occurs. Recently, we have analyzed in detail the LLS to ELS transition of the fiber bundle model on Watts–Strogatz networks and its dependence on the amount of strength disorder of fibers.[47] Based on the behavior of the macroscopic strength of the bundle and the evolution of the size distribution of cascades, we determined the rewiring probability p_l of the onset of the transition as a function of the Weibull exponent m.[47] In particular, for $m = 1.5, 3, 5$, the values $p_l \approx 0.032, 0.08, 0.11$, and $p_u \approx 0.13, 0.23, 0.52$ were obtained numerically for the lower and upper bounds, respectively. The behavior of the cascade duration, i.e., the evolution of the exponent τ_W and the cutoff value $W_{\max}$ of the duration distribution, revealed by the present study follows the overall evolution of the size distribution of cascades, and hence, it is consistent with the LLS to ELS transition.[47]

Comparing the curves of the exponents τ and τ_w at two different Weibull parameters $m = 1.5$ and $m = 3$ in Fig. 6, it can be inferred that the amount of disorder of the strength of fibers plays a crucial role in the evolution of the statistics of cascades during the LLS to ELS transition: outside the ELS regime $p < p_u(m)$, the exponents τ and τ_W are not universal, i.e., at lower disorder (higher m) both exponents get larger, while their difference decreases. However, with increasing p, the exponents τ and τ_W obtained at different Weibull exponents m converge toward the same mean field values τ^{ELS} and τ_W^{ELS}, which are universal. As the strength disorder gets reduced with increasing m, the rewiring probability p_l of the onset of the transition shifts to higher values and the upper bound p_u of the transition regime also increases. It is interesting to note that the exponents τ and τ_W have a well-defined minimum at a rewiring probability $p^*(m)$. The result implies that the network topology obtained at p^* provides the highest stability where the system can tolerate the largest cascades without collapsing. With decreasing strength disorder (increasing m), the transition from the LLS to the ELS universality class becomes more abrupt and the local minimum of the exponents gets sharper and deeper compared to the limit values at $p \to 1$.

Figure 7 demonstrates that the average largest burst size $\langle \Delta_{\max} \rangle$ and largest duration $\langle W_{\max} \rangle$ exhibit qualitatively the same evolution as the exponents τ and τ_W with increasing rewiring probability p. Both cutoffs are increasing functions of p for each Weibull exponent m which implies that at higher structural randomness networks can tolerate cascades with longer duration and larger size. However, the size of cascades increases faster than the duration, which indicates that sub-cascades are getting larger with increasing p. Note that as the strength disorder decreases with increasing m, at low p values, the difference of $\langle \Delta_{\max} \rangle$ and $\langle W_{\max} \rangle$ gradually disappears. This shows that sub-cascades typically consist of one to two breaking fibers in this parameter range, however, with increasing rewiring probability the difference between the two curves gets again higher.

Of course, at a given parameter set, avalanches of longer duration have a larger size but the details of the relation of the two quantities can depend both on the network structure of the load transmitting connections and the amount of strength disorder of nodes (fibers). To quantify this relation, we determined the average size of cascades $\langle \Delta \rangle$ with a fixed duration W. Figure 8(a) demonstrates for the Weibull parameter $m = 3$ that at each value of the rewiring probability p, the average cascade size $\langle \Delta \rangle$ increases as a power law of the duration,

$$\langle \Delta \rangle \sim W^{\beta}. \tag{8}$$

However, the exponent β depends on the value of p. At low p in the range $p < p_l$, where the failure dynamics is close to the LLS class, the cascade size slowly increases with the duration so that $\beta = 1.3 \pm 0.08$ was obtained by fitting. For larger p values $p > p_l$ where long range connections start to dominate the spreading of cascades, a crossover can be observed: small avalanches, which are not affected by the rewired contacts, are still characterized by the LLS value of β. However, beyond a characteristic duration W_c, a steeper increase sets on with a higher exponent, which gradually increases with the rewiring probability. In the limit of $p \to 1$, we obtained $\beta = 1.78 \pm 0.12$, which falls close to the corresponding mean field value $\beta^{ELS} \approx 2$. For lower strength disorder of fibers $m = 5$ in Fig. 8(b) qualitatively, the same behavior is obtained, however, similar to the exponents of cascade size τ and duration τ_W, the value of β proved to be universal only in the mean field limit attained in the range of the rewiring probability $p > p_u$. On networks obtained at lower structural randomness $p < p_u$, the exponent β depends on the amount of strength disorder of fibers controlled by m. In particular, in Fig. 8(b), we obtained $\beta = 1.77$ for $p = 1$, while in the LLS universality class $p = 0$, the exponent is $\beta = 1.1$ significantly lower than for $m = 3$. To make the effect of the amount of strength disorder more transparent, we determined the exponent β by the careful fitting of the $\langle \Delta \rangle(W)$ curves at each p value. The results are summarized in Fig. 8(c) where β is presented as a function of p for four different values of the Weibull exponent m. Note that the overall behavior of the curves is consistent with the outcomes of the analysis of the probability distributions of the size and duration of cascades. In the mean field limit $p > p_u(m)$ the value of β is practically the same for all m within the error bars $\sigma_\beta \approx 0.1$. As the strength disorder gets reduced by increasing m, the LLS value of β decreases and tends to 1, which confirms that at low strength, disorder sub-cascades consist of mainly single breaking fibers so that the cascade size increases linearly with the duration.

Of course, the three exponents β, τ, and τ_W of the cascade size and duration are not independent, one can easily show that the scaling relation

$$\beta = \frac{\tau_W - 1}{\tau - 1} \tag{9}$$

must hold among them.[18,48] As an example, Fig. 8(d) presents the two sides of Eq. (9) as a function of the rewiring probability p for $m = 3$. A reasonable agreement is obtained between the two curves which confirms the consistency of the numerical results. Our computer simulations revealed that the scaling relation Eq. (9) is valid at any amount of strength disorder controlled by the Weibull exponent m and on all network topologies. Note that in the limit of very

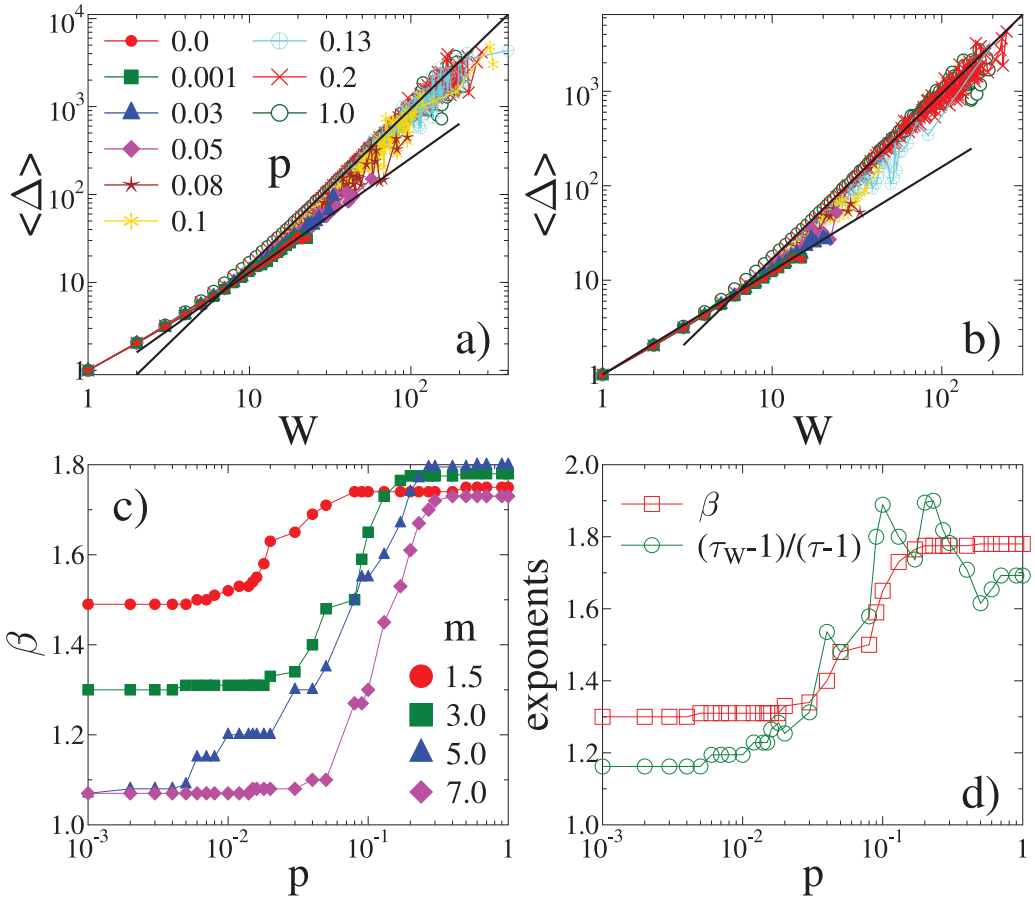

FIG. 8. The average size of cascades $\langle\Delta\rangle$ as a function of their duration W for several values of the rewiring probability p at the disorder exponents $m = 3$ (a) and $m = 5$ (b). The continuous straight lines represent power laws of exponents 1.3, 1.78 and 1.1, 1.77 in (a) and (b), respectively. (c) The exponent β as a function of the rewiring probability for several values of the Weibull exponent m. (d) Test of the scaling relation Eq. (9) for $m = 3$. A reasonable agreement can be observed between β and the value of the expression $(\tau_W - 1)/(\tau - 1)$.

low disorder $m \gg 1$ as β tends to 1 in the LLS universality class, the exponents of the cascade size and duration must approach the same limit values so that $\tau_W = \tau$ follows for $p < p_l(m)$.

IV. TEMPORAL PROFILE OF SPREADING CASCADES

Cascades evolve through a sequence of sub-cascades whose size Δ_s can have strong fluctuations. This is illustrated in Fig. 9 which presents the temporal evolution $\Delta_s(u)$ $(u = 1, \ldots, W)$ of three cascades with a fixed duration $W = 57$ on a network at the rewiring probability $p = 0.5$. It can be observed that the temporal profile $\Delta_s(u)$ of single cascades is a stochastic curve; however, simulations revealed that averaging over cascades of a fixed duration the average profile $\langle\Delta_s(u)\rangle$ has a well-defined functional form which is parabolic (see Fig. 9).

To give a quantitative characterization of the temporal evolution of cascades on different network topologies, we analyzed profiles $\langle\Delta_s(u, W)\rangle$ of cascades averaged over a large number of events of the same duration W at a given parameter set of the fiber bundle. Figure 10 compares cascade profiles of the same duration W at different values of the rewiring probability p. It can be observed that as p increases, the size of sub-cascades increases so that cascades grow to larger sizes Δ at the same value of W. The result implies that due to the presence of long range connections cascades of the same duration spread over a larger area in the bundle without becoming unstable. Note that at all p values and durations W, the profiles have a parabolic shape with a certain degree of right handed asymmetry. Since the size of sub-cascades is the rate of increase of the cascade size, the asymmetry indicates that the spreading of failure cascades starts slowly then accelerates and eventually stops suddenly. It can be inferred from Fig. 10 that the highest asymmetry is obtained on the regular square lattice $p = 0$, which then gets reduced with increasing rewiring probability p. It is important to emphasize that the asymmetry prevails even in the limit $p \to 1$, when the load transmission network becomes completely randomized. The degree of asymmetry proved to be characteristic of the structure of the network in

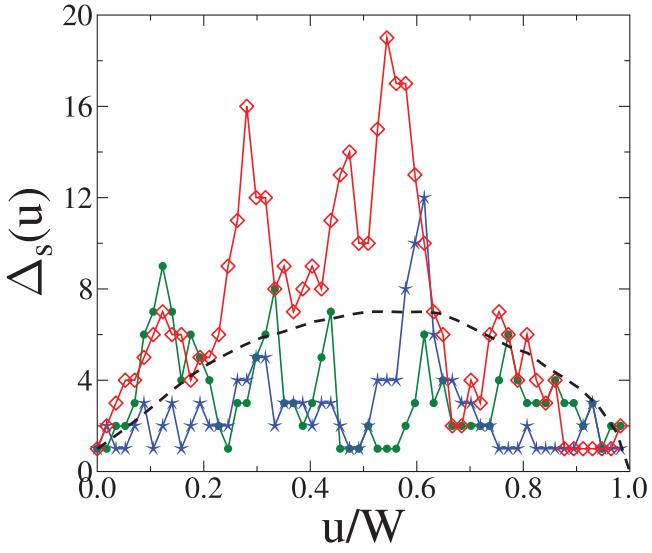

FIG. 9. The evolution of single cascades at the rewiring probability $p = 0.5$. The size of sub-cascades $\Delta_s(u)$ is presented for three cascades of duration $W = 57$ in such a way that the time variable u is rescaled with W. The dashed line presents the temporal profile averaged over 150 events of the same duration.

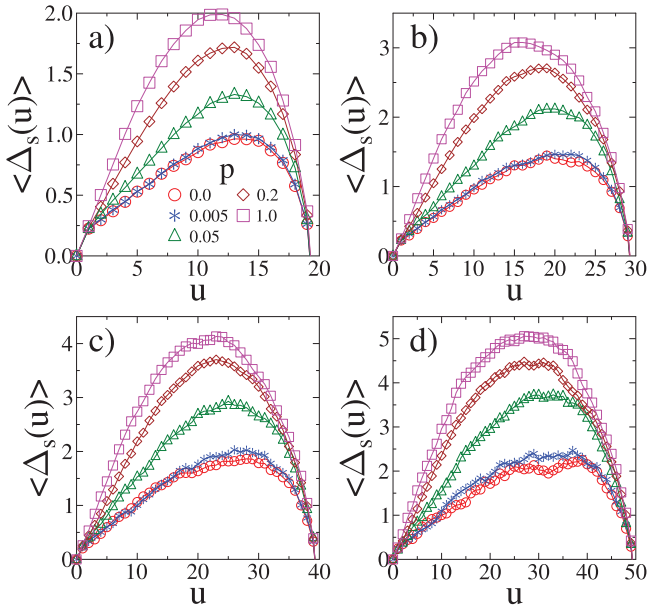

FIG. 10. Temporal profile of failure cascades $\langle\Delta_s(u, W)\rangle$ obtained by averaging over a large number of cascades of the same duration W for the Weibull exponent $m = 1.5$. Profiles of the same W are compared at different values of the rewiring probability p for several W: (a) 20, (b) 30, (c) 40, and (d) 50.

the sense that at a given rewiring probability p, it has the same value for all the cascades irrespective of the duration W. This is demonstrated in Fig. 11 for $m = 1.5$, where rescaling the cascade profiles $\langle\Delta_s(u, W)\rangle$ with an appropriate power α of W and the profiles of different durations W collapse on top of each other. The good quality data collapse implies the validity of the scaling structure of profiles,

$$\langle\Delta_s(u, W)\rangle = W^{\alpha} f(u/W), \tag{10}$$

where both the exponent α and the scaling function $f(x)$ depend on the network structure p. The value of α falls between 0.65 and 1 in the figure. The scaling analysis makes it even more transparent that cascade profiles of random graphs $p = 1$ are not symmetric [see Fig. 11(d)] in spite of the symmetric parabolic pulse shape of avalanches in equal load sharing fiber bundles.[13,49]

In order to give a quantitative characterization of the evolution of the degree of asymmetry with the rewiring probability p, we fitted the scaling function $f(x)$ with the expression

$$f(x) \sim [x(1-x)]^{\alpha}\,[1 - a(x - 1/2)]\,, \tag{11}$$

which has been proposed in Ref. 18 based on the experimental investigation of interfacial crack propagation. Note that the parameter α is the same as in Eq. (10). The degree of anisotropy is controlled by the value of the parameter a in such a way that $a = 0$ means symmetry, while negative and positive values characterize right and left handed asymmetry, respectively. It can be observed in Fig. 11 that Eq. (11) provides a good quality fit of the scaling functions $f(x)$ at all p values.

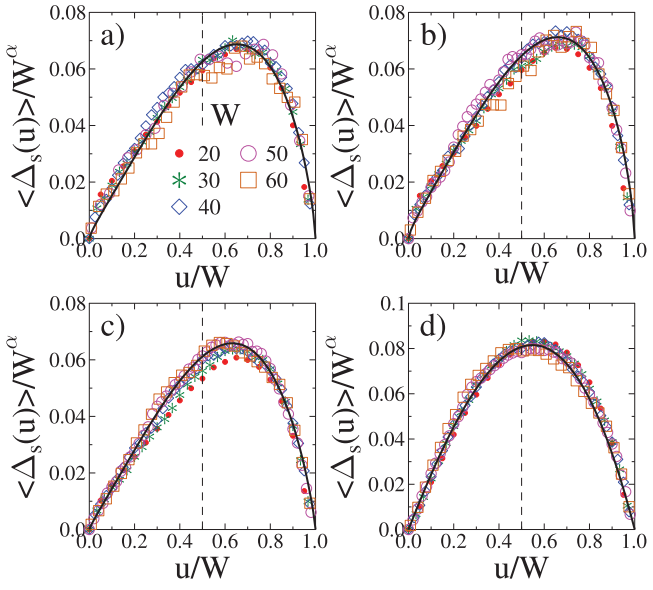

FIG. 11. Scaling analysis of the temporal profile of cascades at fixed values of the rewiring probability p: (a) 0, (b) 0.005, (c) 0.05, and (d) 1 for $m = 1.5$. Rescaling the profiles $\langle\Delta_s(u, W)\rangle$ with an appropriate power α of W, cascades of different durations can be collapsed on the top of each other. The vertical dashed lines indicate the position of the middle point of the interval [0, 1]. The continuous bold lines were obtained by fitting the scaling function with Eq. (11).

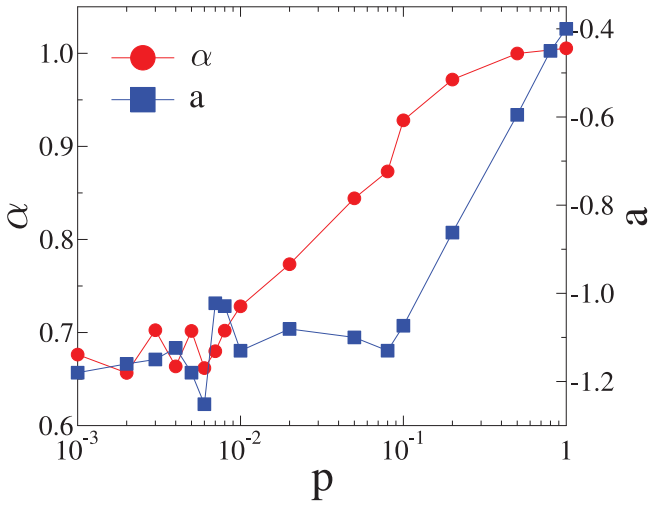

FIG. 12. Shape parameters of avalanche profiles α (left axis) and a (right axis) for $m = 1.5$.

Figure 12 presents how the exponent α and the asymmetry parameter a depend on the rewiring probability p for the Weibull exponent $m = 1.5$. The value of α controls how flat the profile is around its maximum and how rounded the curve is around the ending points $u/W = 0$ and $u/W = 1$ without any effect on the symmetry. The closer α is to 1, the more parabolic the profile shape is.[13,18,49] Moreover, the parameter a mainly affects the position of the maximum without modifying the overall shape of the profile curves. It can be observed in the figure that the exponent α increases starting from the vicinity of 0.65 at $p = 0$ to 1 at $p = 1$, which shows that the cascade profile approaches the simple parabolic form of ELS bundles as the load transmission network gets randomized. However, the asymmetry parameter increases from $a \approx -1.0$ to $a \approx -0.4$ with increasing p so that even at $p = 1$, it remains negative, indicating that some degree of asymmetry prevails on the fully random network. Note that the evolution of α with the rewiring probability p is qualitatively similar to the behavior of the other exponents β, τ, and τ_W showing the LLS to ELS transition. However, the value of the asymmetry parameter a remains constant keeping its LLS value approximately up to the upper bound of the transition regime p_u and then it continuously increases until $p = 1$ is reached. The scaling law equation (10) implies that the average avalanche size $\langle\Delta\rangle$ increases as a power law of the duration $\langle\Delta\rangle \sim W^{1+\alpha}$, as it has been expressed in Eq. (8). It follows that the two exponents α and β have the simple relation $\beta = 1 + \alpha$. Comparing the values of α and β obtained from the scaling function in Eq. (11) and by fitting the average cascade size as a function of the duration in Fig. 8, respectively, the above relation holds to a good precision.

The scaling analysis of the average temporal profile of failure cascades requires a large number of cascades at relatively high durations. However, as the strength disorder of fibers is decreased by increasing the Weibull exponent m, the distribution of both the size and the duration of cascades becomes steeper, which drastically reduces the number of large cascades of long duration, and, hence, it prevents the profile analysis at low disorder. This is the reason why results on cascade profiles are presented only for a single m value in the range of high disorder.

V. DISCUSSION AND CONCLUSIONS

We presented a detailed study of the spreading dynamics of failure cascades in the fiber bundle model focusing on the role of the structure of the underlying load transmission network and the amount of disorder of fibers' strength. Under a slowly increasing external load, fibers fail when the local load exceeds their strength, which is a random variable sampled from a Weibull distribution. After a failure event, the load dropped by the broken fiber is redistributed locally over its intact nearest neighbors along the links of the network of load transmitting connections. The network is generated starting from a square lattice of fibers, which is then rewired using the Watts–Strogatz rewiring technique. Varying the rewiring probability between 0 and 1, the structure of the network is tuned from completely regular to random. In the model, single breaking events trigger failure cascades that spread on the network in a sequence of breaking and load redistribution steps until they either stop or destroy the entire system. We characterized single cascades by their duration and size, which are the total number of breaking-load sharing steps and the total number of fibers breaking in the cascade, respectively.

We demonstrated that the network structure controlled by the rewiring probability has a strong effect on the statistics of cascades: on the regular lattice $p = 0$, both duration W and size Δ of cascades have power law distributions with relatively high exponents τ_W, τ and low cutoff values. The result indicates that in the presence of a strong load concentration large cascades of long duration very rarely occur. Reducing the amount of strength disorder by increasing the Weibull exponent m, both exponents τ_W and τ increase and they tend toward a common limit value.

The rewiring process introduces long range random connections in the load transmitting network and, hence, reduces the local concentration of load inside the bundle. Consequently, as the rewiring probability p increases, the cascading dynamics of the failure of the bundle undergoes a transition from the localized to the mean field universality class of FBMs. Simulations revealed that the transition sets on at a threshold probability p_l below which all quantities keep their LLS values of $p = 0$. There exists a second threshold p_u of the rewiring probability above which no further changes of the cascade dynamics can be pointed out setting the upper bound of the transition regime. Our results confirm the former findings of Ref. 31 that on complex networks, the behavior of the localized load sharing fiber bundle model becomes identical to the equal load sharing one at a sufficiently high structural randomness. However, we demonstrated that on the micro-level, the transition is accompanied by a complex evolution of the statistical and dynamical features of failure cascades: the exponents of size τ and duration τ_w of the cascade both decrease with the rewiring probability and evolve toward their corresponding mean field values, which are independent of the amount of strength disorder of fibers. Cascades of longer duration have a larger size described by a power law relation with an exponent β.

We showed that at any value of the rewiring probability, the three exponents τ, τ_W, and β obey a scaling relation with a reasonable precision.

Failure cascades always start from a single failing node and gradually spread as the load is redistributed through the transmission network. We demonstrated that at all rewiring probabilities, the average temporal profile of cascades is a distorted parabola with a right handed asymmetry, which implies that cascades start slowly, then accelerate, and stop suddenly. Simulations revealed that as the network gets more and more randomized, cascades of the same duration grow to larger sizes and the degree of asymmetry of their profile decreases. We showed that at a given network topology p, avalanche profiles of different durations can be collapsed on top of each other applying a scaling transformation. The result confirms that the degree of asymmetry is characteristic of the network structure. In the limit of completely random networks, the profiles approach the perfectly symmetric parabolic shape of mean field cascades; however, some asymmetry prevailed. The general scaling relation of the exponent α providing the best collapse of profiles of different durations and the exponent β describing the duration dependence of the cascade size was found to hold to a reasonable precision.

Recently, the average temporal profile of spreading cascades has been analyzed on complex networks by analytical and numerical means in Ref. 9. Using maximally random networks (generated, e.g., by the configuration model[50]), it was shown that asymmetric avalanche profiles typically emerge when the degree distribution is fat-tailed. The asymmetry was found to be left handed, predicting a rapid start and a gradually diminishing deceleration toward stopping. The outcomes of our fiber bundle study may be compared to these findings only in the limit of $p \to 1$. We conjecture that the right handed asymmetry we observe can be attributed to the different degree distributions and to the way of load redistribution. In particular, we think one of the reasons why deviations from the mean field behavior occur even at $p = 1$ is that in the mean field limit of FBMs all fibers interact with all other ones. However, in our system, the average number of interacting partners is fixed to 4 by the rewiring algorithm. Although randomization of the network gradually reduces the locality of load sharing, due to the low number of interacting partners deviations from ELS still remain relevant. The way of load sharing in FBMs, including the constraint of load conservation, may be responsible for the right handed asymmetry of avalanche profiles, i.e., as avalanches propagate the accumulation of load along their front introduces a certain memory effect in the stochastic growth process similar to the mechanism proposed in Ref. 51. Calculations to clarify these important issues are in progress.

In our present study, cascades and sub-cascades were characterized by their size defined as the number of nodes failed during them. Depending on the specific properties of the system under consideration, other quantities may also be interesting to quantify cascades, e.g., in the context of the fracture of heterogeneous materials, the energy realized during an event is easier to measure. Although for equal load sharing the size and energy of cascades are proportional to each other, this is not the case for localized load sharing where novel behavior can be expected. Results in this direction will be presented in a forthcoming publication.

ACKNOWLEDGMENTS

This work was supported by the EFOP-3.6.1-16-2016-00022 project. This research was supported by the National Research, Development and Innovation Fund of Hungary, financed under the K-16 funding scheme (Project No. K 119967). Project No. TKP2021-NKTA-34 has been implemented with support provided from the National Research, Development and Innovation Fund of Hungary, financed under the TKP2021-NKTA funding scheme.

AUTHOR DECLARATIONS

Conflict of Interest

The authors have no conflicts to disclose.

DATA AVAILABILITY

The data that support the findings of this study are available from the corresponding author upon reasonable request.

REFERENCES

[1]S. Boccaletti, V. Latora, Y. Moreno, M. Chavez, and D. Hwang, "Complex networks: Structure and dynamics," Phys. Rep. **424**, 175 (2006).
[2]I. Dobson, B. A. Carreras, V. E. Lynch, and D. E. Newman, "Complex systems analysis of series of blackouts: Cascading failure, critical points, and self-organization," Chaos **17**, 026103 (2007).
[3]Y. Moreno, J. B. Gómez, and A. F. Pacheco, "Instability of scale-free networks under node-breaking avalanches," Europhys. Lett. **58**, 630–636 (2002).
[4]D. Trpevski, W. K. S. Tang, and L. Kocarev, "Model for rumor spreading over networks," Phys. Rev. E **81**, 056102 (2010).
[5]R. Pastor-Satorras, C. Castellano, P. Van Mieghem, and A. Vespignani, "Epidemic processes in complex networks," Rev. Mod. Phys. **87**, 925–979 (2015).
[6]M. E. J. Newman, "Spread of epidemic disease on networks," Phys. Rev. E **66**, 016128 (2002).
[7]M. Barthélemy, "Spatial networks," Phys. Rep. **499**, 1–101 (2011).
[8]I. Dobson, "Estimating the propagation and extent of cascading line outages from utility data with a branching process," IEEE Trans. Power Syst. **27**, 2146–2155 (2012).
[9]J. Gleeson and R. Durrett, "Temporal profiles of avalanches on networks," Nat. Commun. **8**, 3 (2017).
[10]N. Jung, Q. A. Le, K.-E. Lee, and J. W. Lee, "Avalanche size distribution of an integrate-and-fire neural model on complex networks," Chaos **30**, 063118 (2020).
[11]B. Casals and E. K. H. Salje, "Energy exponents of avalanches and Hausdorff dimensions of collapse patterns," Phys. Rev. E **104**, 054138 (2021).
[12]M. Stojanova, S. Santucci, L. Vanel, and O. Ramos, "High frequency monitoring reveals aftershocks in subcritical crack growth," Phys. Rev. Lett. **112**, 115502 (2014).
[13]Z. Danku and F. Kun, "Temporal and spacial evolution of bursts in creep rupture," Phys. Rev. Lett. **111**, 084302 (2013).
[14]J. Rosti, X. Illa, J. Koivisto, and M. J. Alava, "Crackling noise and its dynamics in fracture of disordered media," J. Phys. D: Appl. Phys. **42**, 214013 (2009).
[15]J. P. Sethna, K. A. Dahmen, and C. R. Meyers, "Crackling noise," Nature **410**, 242 (2001).
[16]P. Massobrio, L. de Arcangelis, V. Pasquale, H. J. Jensen, and D. Plenz, "Criticality as a signature of healthy neural systems," Front. Syst. Neurosci. **9**, 00022 (2015).
[17]S. Papanikolaou, F. Bohn, R. L. Sommer, G. Durin, S. Zapperi, and J. P. Sethna, "Universality beyond power laws and the average avalanche shape," Nat. Phys. **7**, 316–320 (2011).
[18]L. Laurson, X. Illa, S. Santucci, K. Tore Tallakstad, K. J. Maloy, and M. J. Alava, "Evolution of the average avalanche shape with the universality class," Nat. Commun. **4**, 242 (2013).

[19]S. Zapperi, C. Castellano, F. Colaiori, and G. Durin, "Signature of effective mass in crackling-noise asymmetry," Nature Phys. **1**, 46–49 (2005).
[20]F. Colaiori, "Exactly solvable model of avalanches dynamics for Barkhausen crackling noise," Adv. Phys. **57**, 287–359 (2008).
[21]F. Colaiori, S. Zapperi, and G. Durin, "Shape of a Barkhausen pulse," J. Magn. Magn. Mater. **272–276**, E533–E534 (2004).
[22]B. Dou, X. Wang, and S. Zhang, "Robustness of networks against cascading failures," Physica A **389**, 2310–2317 (2010).
[23]J. Borge-Holthoefer, R. A. Baños, S. González-Bailón, and Y. Moreno, "Cascading behaviour in complex socio-technical networks," J. Complex Netw. **1**, 3–24 (2013).
[24]S. Siddique and V. Volovoi, "Failure mechanisms of load-sharing complex systems," Phys. Rev. E **89**, 012816 (2014).
[25]J. Awrejcewicz and M. A. F. Sanjuán, "Introduction to focus issue: Recent advances in modeling complex systems: Theory and applications," Chaos **31**, 070401 (2021).
[26]D. V. Stäger, N. A. M. Araújo, and H. J. Herrmann, "Usage leading to an abrupt collapse of connectivity," Phys. Rev. E **90**, 042148 (2014).
[27]R. C. Hidalgo, F. Kun, K. Kovács, and I. Pagonabarraga, "Avalanche dynamics of fiber bundle models," Phys. Rev. E **80**, 051108 (2009).
[28]A. Hansen, P. Hemmer, and S. Pradhan, *The Fiber Bundle Model: Modeling Failure in Materials*, Statistical Physics of Fracture and Breakdown (Wiley, 2015).
[29]B. K. Chakrabarti, S. Biswas, and S. Pradhan, "Cooperative dynamics in the fiber bundle model," Front. Phys. **8**, 499 (2021).
[30]F. Kun, F. Raischel, R. C. Hidalgo, and H. J. Herrmann, "Extensions of fiber bundle models," in *Modelling Critical and Catastrophic Phenomena in Geoscience: A Statistical Physics Approach*, Lecture Notes in Physics, edited by P. Bhattacharyya and B. K. Chakrabarti (Springer-Verlag, Berlin, 2006), pp. 57–92.
[31]D.-H. Kim, B. J. Kim, and H. Jeong, Universality class of the fiber bundle model on complex networks," Phys. Rev. Lett. **94**, 025501 (2005).
[32]U. Divakaran and A. Dutta, "Fibers on a graph with local load sharing," Int. J. Mod. Phys. C **18**, 919 (2011).
[33]Z. Domanski, "Spreading of failures in small-world networks: A connectivity-dependent load sharing fibre bundle model," Front. Phys. **8**, 441 (2020).
[34]O. Yağan, "Robustness of power systems under a democratic-fiber-bundle-like model," Phys. Rev. E **91**, 062811 (2015).
[35]J. M. Reynolds-Barredo, D. E. Newman, B. A. Carreras, and I. Dobson, "The interplay of network structure and dispatch solutions in power grid cascading failures," Chaos **26**, 113111 (2016).
[36]S. Biswas and L. Goehring, "Load dependence of power outage statistics," Europhys. Lett. **126**, 44002 (2019).
[37]C. Barré and J. Talbot, "Cascading blockages in channel bundles," Phys. Rev. E **92**, 052141 (2015).
[38]B. K. Chakrabarti, "A fiber bundle model of traffic jams," Physica A **372**, 162–166 (2006).
[39]J.-F. Zheng, Z.-Y. Gao, X.-M. Zhao, and B.-B. Fu, "Extended fiber bundle model for traffic jams on scale-free networks," Int. J. Mod. Phys. C **19**, 1727–1735 (2011).
[40]D. Watts and S. Strogatz, "Collective dynamics of 'small-world' networks," Nature **393**, 440–442 (1998).
[41]D. J. Watts, "Networks, dynamics, and the small-world phenomenon," Am. J. Sociol. **105**, 493–527 (1999).
[42]V. Latora, V. Nicosia, and G. Russo, *Complex Networks—Principles, Methods and Applications* (Cambridge University Press, Cambridge, 2017).
[43]R. C. Hidalgo, Y. Moreno, F. Kun, and H. J. Herrmann, "Fracture model with variable range of interaction," Phys. Rev. E **65**, 046148 (2002).
[44]F. Raischel, F. Kun, and H. J. Herrmann, "Local load sharing fiber bundles with a lower cutoff of strength disorder," Phys. Rev. E **74**, 035104 (2006).
[45]Y. Moreno, J. B. Gomez, and A. F. Pacheco, "Fracture and second-order phase transitions," Phys. Rev. Lett. **85**, 2865–2868 (2000).
[46]F. Kun, S. Zapperi, and H. J. Herrmann, "Damage in fiber bundle models," Eur. Phys. J. B **17**, 269 (2000).
[47]A. Batool, G. Pal, Z. Danku, and F. Kun, "Transition from localized to mean field behaviour of cascading failures in the fiber bundle model on complex networks," arXiv:2202.08364 [cond-mat.dis-nn] (2022).
[48]G. Durin and S. Zapperi, "Scaling exponents for Barkhausen avalanches in polycrystalline and amorphous ferromagnets," Phys. Rev. Lett. **84**, 4705 (2000).
[49]Z. Danku, G. Ódor, and F. Kun, "Avalanche dynamics in higher-dimensional fiber bundle models," Phys. Rev. E **98**, 042126 (2018).
[50]M. E. J. Newman, *Networks: An Introduction* (Oxford University Press, Oxford, 2010).
[51]A. Baldassarri, F. Colaiori, and C. Castellano, "Average shape of a fluctuation: Universality in excursions of stochastic processes," Phys. Rev. Lett. **90**, 060601 (2003).